

## Effects of strain rate and temperature on microstructure and texture for AZ31 during uniaxial compression

XIN Ren-long(辛仁龙)<sup>1,2</sup>, WANG Bing-shu(汪炳叔)<sup>1</sup>, ZHOU Zheng(周正)<sup>1</sup>,  
HUANG Guang-jie(黄光杰)<sup>1,2</sup>, LIU Qing(刘庆)<sup>1,2</sup>

1. College of Materials Science and Engineering, Chongqing University, Chongqing 400044, China;

2. National Engineering Research Center for Magnesium Alloys, Chongqing University, Chongqing 400044, China

Received 23 September 2009; accepted 30 January 2010

**Abstract:** In order to investigate the effects of strain rate and temperature on the microstructure and texture evolution during warm deformation of wrought Mg alloy, AZ31 extruded rods were cut into cylinder samples with the dimension of  $d8\text{ mm}\times 12\text{ mm}$ . The samples were compressed using a Gleeble 1500D thermo-mechanical simulation machine at various strain rates (0.001, 0.01, 0.1, 1 and  $5\text{ s}^{-1}$ ) and various temperatures (300, 350, 400 and  $450\text{ }^{\circ}\text{C}$ ). The microstructure and texture of the compressed samples at the same strain under different deformation conditions were studied and compared by electron backscatter diffraction (EBSD) in scanning electron microscope (SEM). The results show that the size of recrystallized grains in the deformed samples generally increases with the decrease of strain rate and the increase of temperature. After 50% reduction, most basal planes are aligned perpendicular to the compression direction at relatively high strain rate ( $>0.01\text{ s}^{-1}$ ) or low temperature ( $<350\text{ }^{\circ}\text{C}$ ). The optimized strain rate is  $0.1\text{ s}^{-1}$  for uniaxial compression at  $300\text{ }^{\circ}\text{C}$ , which produces about 80% of small grains ( $<5\text{ }\mu\text{m}$ ).

**Key words:** magnesium alloy; electron backscatter diffraction; dynamic recrystallization; microstructure; texture

### 1 Introduction

Improving fuel economy and reducing emissions of vehicles can be achieved by low density construction. Mg alloys offer a remarkable potential in this regard because of their low density, high specific strength and stiffness, superior damping capacity, high thermal conductivity and good electromagnetic shielding characteristics[1–2]. However, the structural applications of Mg alloys are limited because of their poor deformability by cold working, due to their hexagonal closed-packed (HCP) crystal structure[3]. To improve the forming ability and ductility, wrought Mg alloys are normally processed at warm temperatures. Therefore, it is desirable to understand the thermal deformation behavior of Mg alloys under various deformation conditions.

The flow stress characteristic and microstructure evolution under warm forming process of Mg alloys have been carried out in previous studies[4–6]. For example, MAKSOUD and AHMEO[4] investigated the

effect of strain rate and temperature on the deformability and microstructure evolution of AZ31 Mg alloy and found that at high temperature and low-strain rates the peak stress was reduced while the volume fraction and size of dynamically recrystallized grains were increased. KLIMANEK and POTZSCH[5] studied the microstructure evolution in compression tests of polycrystalline Mg and found it was dependant significantly on the initial state (grain size, texture and dislocation arrangement) of the sample material. The influence of texture on plastic deformation and texture evolution has also been reported[7–9]. However, despite the significant efforts, the microstructure and texture evolution during warm deformation process of Mg alloy have not been fully understood.

In order to investigate the influence of strain rate and temperature on the microstructure and texture of compressed AZ31 Mg alloys, uniaxial compression tests were carried out to understand the deformation behavior in various ranges of strain rate and temperature. Then, the evolution of microstructure and texture including dynamic recrystallization (DRX) during warm deformation

of AZ31 Mg alloy was analyzed by electron backscatter diffraction (EBSD) technique in the scanning electron microscope (SEM).

## 2 Experimental

The starting material was AZ31 (Mg-3%Al-1%Zn) extruded rod. The cylinders with diameter of 8 mm and length of 12 mm were cut from the rod with the cylinder (compression) axis perpendicular to the extrude direction (ED) for compression testing.

Compression tests were carried out using a Gleeble 1500D in a vacuum of 1 mPa. The test conditions employed in this work were various strain rates (0.001, 0.01, 0.1, 1 and  $5 \text{ s}^{-1}$ ) and various temperatures (300, 350, 400 and  $450 \text{ }^\circ\text{C}$ ). After the tests, the deformed samples were water-quenched immediately to prevent any microstructure change. Microstructure and texture investigations were carried out using EBSD orientation mapping on electropolished surfaces along the compression direction. EBSD analysis was carried out on an FEI Nova 400 FEG-SEM equipped with an HKL channel 5 system to gain detailed information on microstructure and texture development.

## 3 Results and discussion

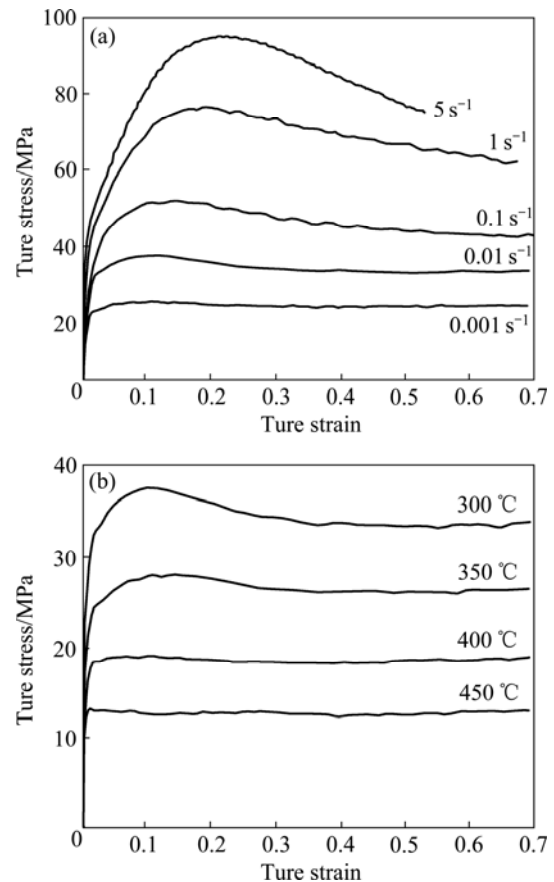
### 3.1 Flow stress behavior

The true stress—strain curves for compression of the samples obtained at various deformation strain rates and temperatures are presented in Figs.1(a) and 1(b), respectively. It can be seen from Fig.1 that the flow stress increases to a peak value and then decreases gradually to finally attain a steady state typically. The decrease of strain after the maximum stress is called strain softening, which has characteristic of the stress—strain curve of Mg alloy, and it is commonly believed that strain softening is attributed to the competition of work hardening and DRX softening. Fig.1 shows that at  $300 \text{ }^\circ\text{C}$ , flow softening is more obvious at higher strain rate, whereas the steady state flow lasts longer at lower strain rates. The flow curves are of steady state right-hand side after the start of plastic deformation at temperatures above  $400 \text{ }^\circ\text{C}$  and strain rates lower than  $0.01 \text{ s}^{-1}$ .

### 3.2 Effects of strain rate on microstructure and texture

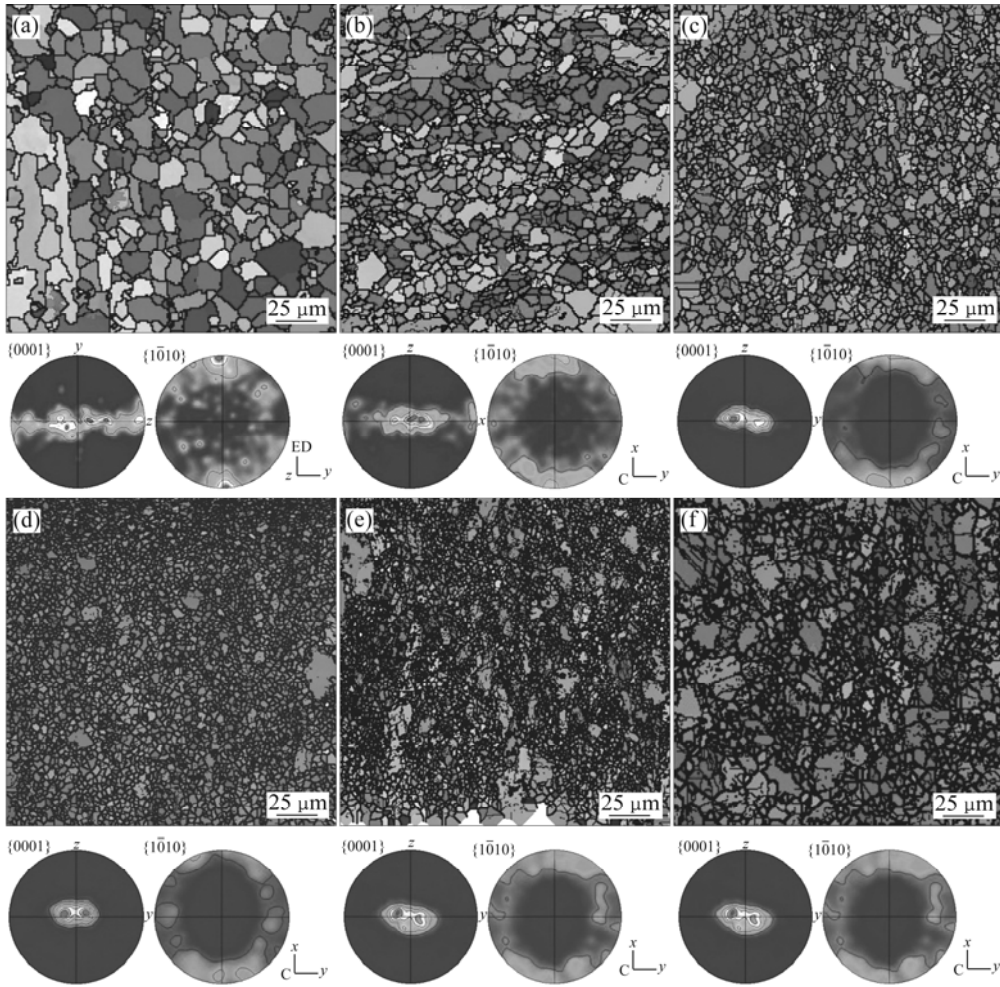
The orientation maps and pole figures obtained from the EBSD data of the initial material and the samples compressed at  $300 \text{ }^\circ\text{C}$  with different strain rates are shown in Fig.2. It can be seen from Fig.2 that thick black lines indicate boundaries above  $15^\circ$  misorientation, and thin lines indicate boundaries between  $2^\circ$  and  $15^\circ$ .

Fig.2(a) shows that the original AZ31 cylinder sample presents a strong fiber texture with the basal plane aligned almost parallel to the extruded direction. After compression, the basal plane gradually reorients towards the compression direction and the basal texture becomes stronger with the increase of the deformation strain rate (Fig.2(b)–2(f)). However, for the samples deformed at strain rate of  $0.001 \text{ s}^{-1}$ , there are also some texture components corresponding to regions with basal planes inclined to the  $y$  direction in addition to basal texture (Fig.2(b)). Fig.2(a) confirms that a few recrystallized grains and elongated grains are presented in the original extruded rod samples after annealing process.



**Fig.1** True stress — strain curves obtained at various deformation conditions of AZ31 after being compressed to 50%: (a) Various strain rates at  $300 \text{ }^\circ\text{C}$ ; (b) Various temperatures at strain rate of  $0.01 \text{ s}^{-1}$

It is revealed that the grain size and homogeneity of the samples are largely influenced by the strain rate of compression. Fig.2(b) shows that the sample deformed at strain rate of  $0.001 \text{ s}^{-1}$  exhibits a comparatively coarse, homogeneous and equiaxed microstructure and no twins are seen in it. It is evident that most grains are recrystallized and the originally deformed grains are depleted by the DRX grains. For the samples compressed at strain rate of 0.01 and  $0.1 \text{ s}^{-1}$ , significant grain refinement is noticed with the increase of strain rate, as



**Fig.2** EBSD maps of AZ31 samples compressed at various strain rates and at 300 °C after 50% reduction: (a) Initial; (b) 0.001 s<sup>-1</sup>; (c) 0.01 s<sup>-1</sup>; (d) 0.1 s<sup>-1</sup>; (e) 1 s<sup>-1</sup>; (f) 5 s<sup>-1</sup> (Contour densities for {0001} pole figures are (2, 4, 6, 8, 10, 12) × random)

shown in Figs.2(c) and 2(d).

A mixed microstructure of a few coarse deformed grains separated by wide regions with finer DRX grains was observed for the sample deformed at a strain rate of 1 s<sup>-1</sup>. While at relatively high strain rate of 5 s<sup>-1</sup>, most grains are coarse deformed grains and with few small recrystallized grains surrounding them, implying apparent suppression of DRX due to the increase of strain rate. This is probably because the severity of dislocation pile-up is increased with the increase of strain rate, so the stress concentration is difficult to relax and DRX is depressed.

In order to understand the effect of strain rate on the distribution of grain size, the area of the grains with various grain sizes was calculated based on the EBSD data, and the result is shown in Fig.3. It can be clearly seen that the deformed samples with strain rate of 0.1 s<sup>-1</sup> produces the most small grains (<5 μm, about 80%) and the least large grains (>15 μm, 0%). In this regard, the strain rate of 0.1 s<sup>-1</sup> shows the highest efficiency for

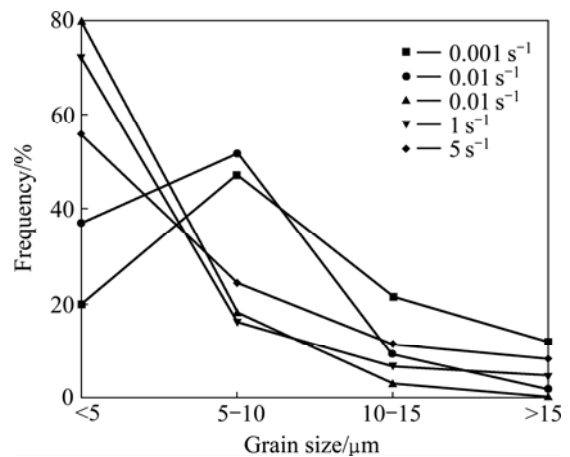


**Fig.3** Effect of strain rate on distribution of grain size in deformed AZ31 Mg alloy at various strain rates and at 300 °C

grain refinement. The strain rate of 1 s<sup>-1</sup> takes the second place. This also indicates that the grain size of the deformed samples with strain rates of 0.001 s<sup>-1</sup> and 0.01 s<sup>-1</sup> ranges mainly in 5–10 μm. The above analyses are consistent with the orientation shown in Fig.2.

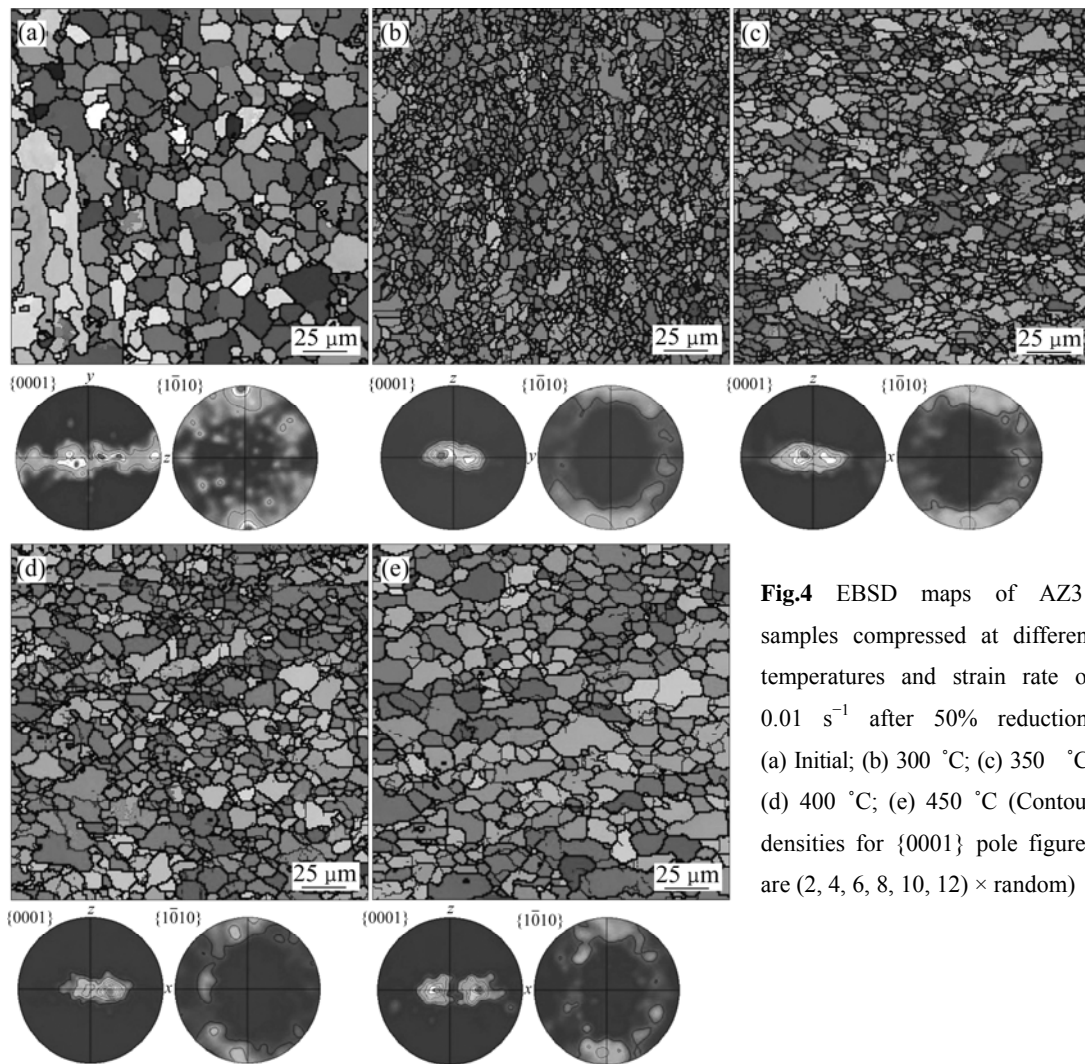


**Fig.4** EBSD maps of AZ31 samples compressed at different temperatures and strain rate of  $0.01 \text{ s}^{-1}$  after 50% reduction: (a) Initial; (b) 300 °C; (c) 350 °C; (d) 400 °C; (e) 450 °C (Contour densities for {0001} pole figures are (2, 4, 6, 8, 10, 12)  $\times$  random)

### 3.3 Effects of temperature on microstructure and texture

The orientation maps and pole figures obtained from the EBSD data of the initial material, and of the samples compressed at a strain rate of  $0.01 \text{ s}^{-1}$  with different temperatures are shown in Fig.4. The microstructure after deformation above 300 °C is characterized by recrystallized equiaxial grains and the grain size gradually increases with the increase of the deformation temperature. Small fine DRX grains are dominant for the samples compressed at 300 °C, whereas a mixed microstructure of many coarse recrystallized equiaxial grains separated by a few finer DRX grains is observed at above 350 °C.

Fig.4 shows that all the deformed samples exhibits approximately basal texture after 50% reduction but with different densities. For the samples deformed at 300 °C, most basal planes are aligned perpendicular to the compression direction. However, for the samples deformed above 350 °C, some texture components

corresponding to regions with basal planes inclined to y direction are presented, implying not only basal slip but also non-basal slip are activated during the deformation[10].

## 4 Conclusions

1) The strain rate and temperature have significant influence on the microstructure and texture evolution during uniaxial compression of AZ31 Mg alloy.

2) The size of recrystallized grains in the deformed samples increases with the decrease of strain rate and the increase of temperature. After 50% reduction, most basal planes are aligned perpendicular to the compression direction at relatively high strain rate ( $>0.01 \text{ s}^{-1}$ ) or low temperature ( $<350 \text{ °C}$ ).

3) The optimized strain rate is  $0.1 \text{ s}^{-1}$  for uniaxial compression at 300 °C, which produces about 80% of small grains ( $<5 \text{ μm}$ ).

## References

- [1] MWEMBELA A, KONOPLEVA E B, MCQUEEN H J. Microstructural development in Mg alloy AZ31 during hot working [J]. *Scripta Mater*, 1997, 37: 1789–1795.
- [2] GALIYEV A, KAIBYSHEV R, GOTTSTEIN G. Correlation of plastic deformation and dynamic recrystallization in magnesium alloy ZK60 [J]. *Acta Mater*, 2001, 49: 1199–1207.
- [3] YANG P, YU Y, CHEN, L. Experimental determination and theoretical prediction of twin orientations in magnesium alloy AZ31 [J]. *Scripta Mater*, 2004, 50: 1163–1168.
- [4] MAKSOUD I A, AHMED H. Investigation of the effect of strain rate and temperature on the deformability and microstructure evolution of AZ31 magnesium alloy [J]. *Materials Science and Engineering A*, 2009, 504: 40–48.
- [5] KLIMANEK P, POTZSCH A. Microstructure evolution under compressive plastic deformation of magnesium at different temperatures and strain rates [J]. *Materials Science and Engineering A*, 2002, 324: 145–150.
- [6] TAN J C, TAN M J. Dynamic continuous recrystallization characteristics in two stage deformation of Mg-3Al-1Zn alloy sheet [J]. *Materials Science and Engineering A*, 2003, 339: 124–132
- [7] JIANG J, GODFREY A, LIU Q. Microtexture evolution via deformation twinning and slip during compression of magnesium alloy AZ31 [J]. *Materials Science and Engineering A*, 2008, 483/484: 576–579
- [8] STYCZYNSKI A, HARTIG CH, BOHLEN J. Cold rolling textures in AZ31 wrought magnesium alloy [J]. *Scripta Mater*, 2004, 50: 943–947.
- [9] BARNETT M R, NAVE M D, BETTLES C J. Deformation microstructures and textures of some cold rolled Mg alloys [J]. *Materials Science and Engineering A*, 2004, 386: 205–211.
- [10] YOO M H, AGNEW S R, MORRIS J R. Non-basal slip systems in HCP metals and alloys: Source mechanisms [J]. *Materials Science and Engineering A*, 2001, 319: 87–92.

(Edited by CHEN Can-hua)